Using a Variable-Friction Robot Hand to Determine Proprioceptive Features for Object Classification During Within-Hand-Manipulation

Adam J. Spiers, *Member, IEEE*, Andrew S. Morgan, *Student Member, IEEE*, Krishnan Srinivasan, Berk Calli, *Member, IEEE*, and Aaron M. Dollar, *Senior Member, IEEE*

***Abstract*—Interactions with an object during within-hand manipulation (WIHM) constitutes an assortment of gripping, sliding, and pivoting actions. In addition to manipulation benefits, the re-orientation and motion of the objects within-the-hand also provides a rich array of additional haptic information via the interactions to the sensory organs of the hand. In this article, we utilize variable friction (VF) robotic fingers to execute a rolling WIHM on a variety of objects, while recording 'proprioceptive' actuator data, which is then used for object classification (i.e., without tactile sensors). Rather than hand-picking a select group of features for this task, our approach begins with 66 general features, which are computed from actuator position and load profiles for each object-rolling manipulation, based on gradient changes. An Extra Trees classifier performs object classification while also ranking each feature's importance. Using only the six most-important 'Key Features' from the general set, a classification accuracy of 86% was achieved for distinguishing the six geometric objects included in our data set. Comparatively, when all 66 features are used, the accuracy is 89.8%.**

***Index Terms*—Robotics, end effectors, manipulators, machine learning, robot learning, robot sensing sytems, haptic sensing, in-hand-manipulation, object identification, robot manipulation.**

I. Introduction

IT is easy to take for granted the wide range of manipulation actions that people make use of in their daily lives. Something as simple as using a touch-screen smartphone one-handed, or removing a credit card from a wallet and inserting into an ATM, involves gripping, sliding and re-orientation of objects. Central to this capability is the sensory facilities of the fingers. Reaching into a pocket and being able to distinguish coins from keys involves complex sensing capabilities tied to active hand and finger motions that enhance perception. Exploratory Procedures (EPs) are the classic embodiment of hand-based interactions that humans complete to extract particular haptic properties from objects [1]. Over a number of years many researchers have looked at the potential of applying exploratory procedures to robotic systems, using a variety of hardware platforms and tactile sensors [2]–[5]. For example, in [6], a robot picked up and pushed objects to determine their weight and resistance to motion. Rather than such large manipulation actions that require the motion of the whole robotic arm, in our work we are more specifically interested in the haptic data that may be obtained via Within-Hand-Manipulation (WIHM) of objects. WIHM, which is also known as In-Hand-Manipulation, is defined in [7] as producing motion of an object within the hand (i.e., in a grasp) via parts of the hand moving with respect to a frame fixed at the base of a hand. Such object motion is classified as 'dexterous manipulation' via the resulting rotational or translational object motions.

WIHM has proven to be a difficult task for robotic and prosthetic hands, with past attempts to achieve WIHM relying on complex dynamic/quasi-static models [8]–[11] of the hand-object system and/or high-DOF robotic hardware [12]–[16]. Recently we have developed novel variable friction (VF) robotic fingers that are able to significantly change the effective coefficient of friction of their contact surface (Fig. 1). Using the VF fingers in a simple 2-DOF gripper configuration with a simple controller, we have demonstrated that the fingers can enable selective gripping, rolling and sliding of an object maintained in a stable grasp [17].

In this current paper we use the same platform to demonstrate how these WIHM actions with the VF fingers can be used to classify object geometries via machine-learning techniques. We achieve this with minimum sensing requirements, i.e., utilizing only the proprioceptive data from the robot actuators (i.e., position and load), rather than any tactile or vision sensor data. Furthermore, to negate the need for hand-selected features, we implement a technique where 66 general features are automatically computed from each manipulation action at predefined events in the data, i.e., at or between sharp gradient changes ('elbows') of position demand, position and torque. These general features are then numerically rated with regard to their contribution to classification performance. This process

Manuscript received January 28, 2019; revised October 21, 2019; accepted November 16, 2019. Date of publication December 9, 2019; date of current version August 25, 2020. This work was supported by the National Science Foundation under Grant IIS-1734190. This article was recommended for publication by Associate Editor D. Lee. and Editor AndreAnna McLean upon evaluation of the reviewers' comments. *(Corresponding author: Adam J. Spiers.)*

A. J. Spiers is with the Department of Haptic Intelligence, Max-Planck Institute for Intelligent Systems, Stuttgart 70569, Germany (e-mail: a.spiers@is.mpg.de).

A. S. Morgan and A. M. Dollar are with the Department of Mechanical Engineering and Materials Science, Yale University, New Haven, CT 06520 USA (e-mail: andrew.morgan@yale.edu; aaron.dollar@yale.edu).

K. Srinivasan is with the Department of Computer Science, Stanford University, Stanford, CA 94305 USA (e-mail: krshna@stanford.edu).

B. Calli is with the Computer Science Department, Worcester Polytechnic Institute, Worcester, MA 01609 USA (e-mail: bcalli@wpi.edu).

Digital Object Identifier 10.1109/TOH.2019.2958669

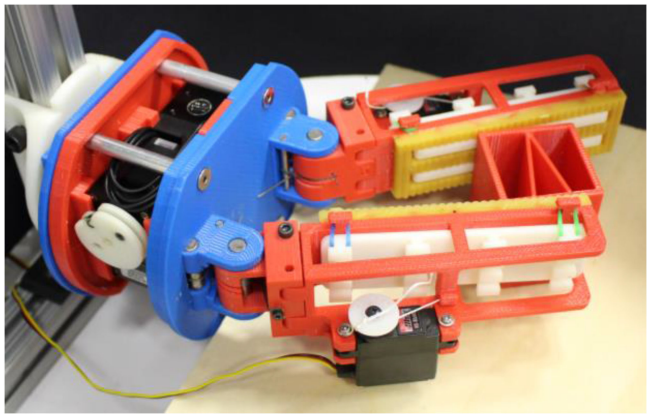

Fig. 1. The robot hand used in this work is composed on two single-link, active variable friction (VF) fingers mounted on a modified Yale OpenHand base. Proprioceptive (position and load) data are collected from the Dynamixel actuators and form the basis of classification.

allows our machine learning system to determine the most important *'key features'* extracted from the WIHM actions to enable efficient object classification.

II. Related Work

In this section we examine haptic exploration and human finger properties in the framework of within-hand-manipulation (WIHM), which is also known as 'in-hand-manipulation'.

A. Within Hand Manipulation

As explained in the previous section, WIHM enables manipulation tasks to be completed without wrist/arm motion or bi-lateral (two-handed) interactions [7]. Resultantly, tasks may be performed faster, with less energy expenditure and in more confined spaces.

Robotic efforts at WIHM have typically led to high-DOF anthropomorphic mechanical systems [13], [14] and/or model-dependent control approaches with in-depth pre-planning and object pose modelling and sensing [9], [10], [18]. Additional efforts have attempted to understand the mechanics of object sliding/slip [19], [20] or rolling [21] to permit emulation of such actions in robotic WIHM. This has led to modelling of frictional effects for dynamic and quasi-static cases [22], [23] and frictional limit surfaces [24]–[26] for various contact assumptions. Low DOF, non-model based approaches to WIHM are also apparent. In [27] an anthropomorphic two-finger gripper design was based on kinematic observations of human hand motion during WIHM translation and re-orientation tasks. Non-anthropomorphic gripper designs to optimize object re-orientation are also present in [28]. In [29] a simple 2 DOF manipulator was combined with an iterative learning approach to establish object re-orientation control schemes. Compared to these other designs, the hand with VF fingers used in this work allows us to exploit various contact friction configurations in much simpler way. This design aims to simplify models required for WIHM, and enable dexterity by adapting the gripper's frictional properties according to desired manipulation actions.

B. Haptic Exploration

Not only does WIHM potentially simplify many manipulation actions, but WIHM actions facilitate the acquisition of rich haptic sensory information via the process of active exploration and 'exploratory procedures' [1]. Rather than the limited tactile data information resulting from a light touch or single grasp [30], [31], exploratory procedures involve dedicated patterns of manipulation, such as squeezing objects to detect their stiffness, or rubbing a surface to detect texture. These procedures are often fluidly combined to extract multiple properties [32].

Exploratory procedures are often defined based on the pioneering work of Lederman and Klatzky, who illustrated eight distinct EPs [1]. It is worth noting that six of the original Eps show bi-manual object interaction, while WIHM tends to focus on a single hand. In [32], study participants were observed combining EPs into efficient compound motions when palpating unknown objects for feature extraction with a single hand. Additionally, in [33] it was noted that adaptive grasping/molding of the human hand around objects facilitated better haptic object identification.

The ability to determine haptic object properties without vision is appealing in numerous scenarios involving occlusion or poor lighting conditions. As such, various roboticists have attempted to implement exploratory procedures, though these processes often require time consuming palpatory motion sequences and complex and expensive high-DOF manipulators and/or tactile sensors (as summarized in [30]). With the design of the VF fingers and gripper used in this work we aimed for simple hardware that may be re-created by anyone with access to a research-grade 3D printer and approximately $600 for additional components (including actuators, dowel pins and springs).

C. Biological Inspiration / Finger Properties

A variety of disciplines have identified that skin friction plays a key role in human manipulation of objects [34]. In particular, the deformability of the finger pad leads to an increasing contact area as normal force is applied. This contact area is related to the effective co-efficient of friction, which saturates after the application of $\sim$1N of normal force [34]–[36]. By modulating their grasp and force on objects, humans are therefore able to regulate whether objects are gripped by, or slide over, the finger surfaces. This ability to selectively grip and slide has been previously considered as beneficial for haptic exploration [3]. We also believe this capability is central to the highly-dexterous manipulation actions commonly observed in our species. This natural gripping and sliding ability is greatly aided by the anatomical structure of the human finger pad.

The finger pad consists of soft internal fatty tissue, which is contained within a more rigid layer of epidermal skin. The skin layer allows sliding over surfaces with light touch, supporting objects without securing them and enabling active exploration motions used for surface discrimination (i.e., stroking/rubbing) [1], [37]–[39]. Beneath the skin, the soft subcutaneous tissue is able to conform around object geometry, gripping features firmly for pivoting or stabilization when sufficient normal force overcomes the limit of compressibility [21], [40]. This deformation also contributes to haptic identification of object contours and hardness [1].

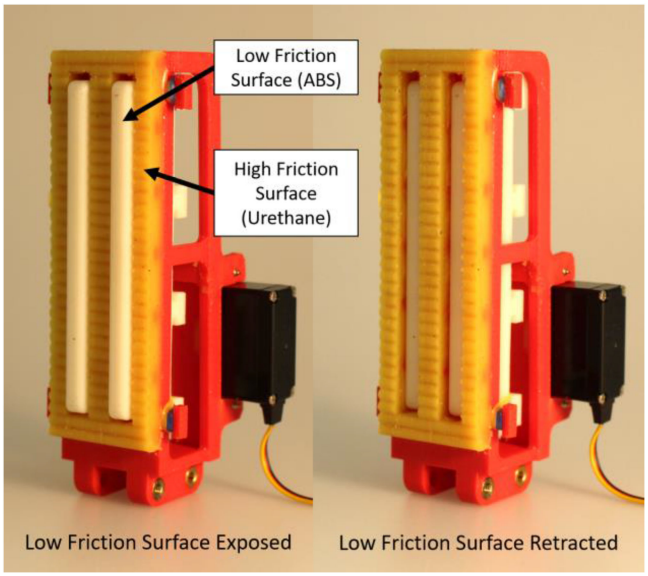

Fig. 2. The variable friction (VF) fingers are composed of a low-friction surface that protrudes through cavities in a high-friction surface. The low-friction surface is suspended with springs and retracts when high-force is applied. A servo motor may also be used to retract the low-friction surface, as in the right image.

Soft, deformable robotic fingers are often implemented in robotic systems and have been shown to be beneficial to establishing grasps, in comparison to rigid systems [21], [41], [42]. Unlike human fingers however, robotic finger pads tend to consist of homogenous rubbers that do not provide the same variety of interaction characteristics as the layered skin and fat of glabrous (smooth & hairless) tissue [41]. Though Chorley *et al*. investigated bio-mimetic multi-material assemblies from cast human fingers, the authors did not implement those fingers in object manipulation [37].

Variable Friction (VF) fingers are a recent development from our lab that use a simple mechanism to achieve a functional analogy to the gripping/sliding behavior of the human finger [17]. In past work we have shown that selectively switching between high and low friction while performing side to side motions of the fingers enables controlled sliding and rolling of objects against the finger surfaces (as illustrated in Fig. 3). The VF fingers will be described in more details in the following section.

III. System Description

A. Mechanical Components

This work makes use of a simple 2DOF robot gripper constructed from a Yale OpenHand base (which has been modified to accommodate two Dynamixel XM430-W350-R actuators) and 2 VF fingers (Fig. 1). These are robot fingers that are able to modify their coefficient of friction using either a passive mechanism (in which an increase in normal force causes an increase in friction) or a mini-servo actuator mounted on each finger, which can convert the fingers from passive VF mode to a constant high-friction mode.

The VF fingers consist of a high-friction deformable finger surface (molded from 'Vytaflex 30' Urethane Rubber) and a low friction, rigid finger surface (made of smooth 3D-printed ABS).

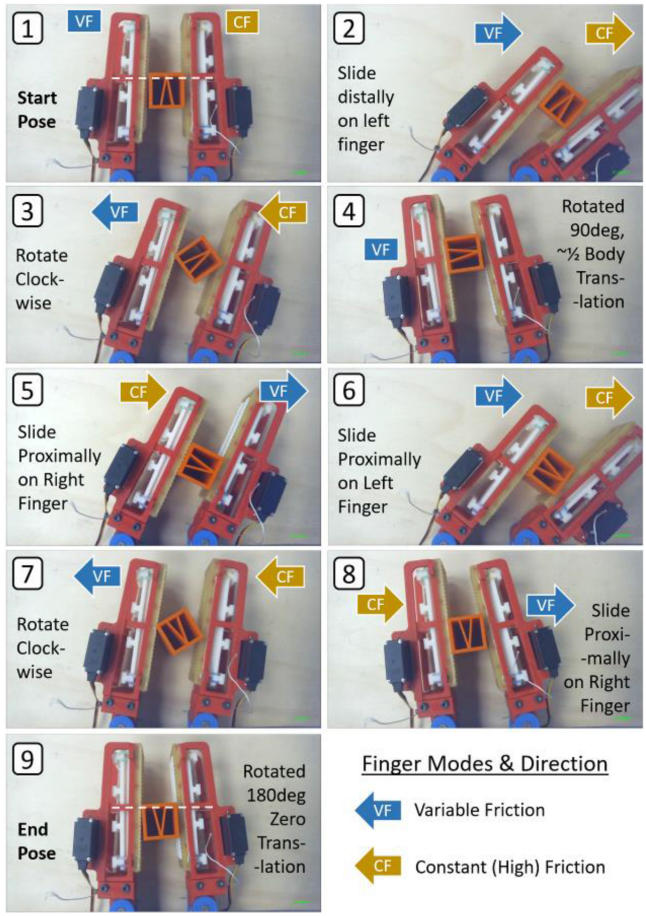

Fig. 3. Variable friction (VF) fingers enable controlled within-hand rotation and translation of objects, despite limited finger dexterity and simple control approach. Here an open-loop control sequence moves an object to a target pose with 180 degree rotation but no translation.

The low friction surface is suspended behind the high-friction surface by means of four elastic dental bands (1/4" 'heavy' variety, manufactured by Essix). This arrangement enables the low friction element's contact surface to protrude through cavities in the high-friction elements contact surface (Fig. 2).

When the VF fingers exert low (<1.2N) normal contact forces on objects, the low friction surface remains exposed, enabling the finger to behave as if it was made of smooth plastic. Once the normal force exceeds that of the elastic elements, the low-friction element is pushed into the cavity of the high-friction element (Fig. 1), exposing the soft and textured high-friction surface. This variation in surface properties allows the contacting finger surface to either slide over objects or grip and pivot them, as in the human finger [27].

The coefficient of static friction for the low and high friction finger surfaces are 0.32 and 0.69 in contact with aluminum and 0.13 and 0.69 in contact with ABS. Modifying the friction surface therefore changes the coefficient by a factor of 2.2 (against aluminum) and 5.5 (against ABS).

The high-friction finger pads are 30 mm wide 95 mm long. The low friction inserts consist of two rectangular sections (5.5 mm wide and 80 mm long) with a separation of 7.5 mm, joined by a common base. These protrude 1.25 mm beyond the ridges of the high-friction surface when no normal force is

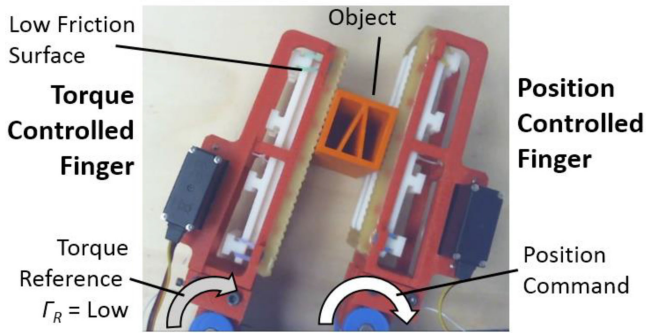

Fig. 4. The hybrid position and torque controlled nature of the end effector enables a stable grasp on objects during WIHM. As such, the torque controlled finger (which switches from the left to right digit depending on direction of object motion) generates different position and load trajectories for each object in relation to the relatively consistent driving motion of the position controlled finger.

applied. Full details of the VF finger fabrication may be found in [17]. The design of these fingers is open source and CAD files for 3d-printing may be downloaded from www.eng.yale.edu/grablab/openhand, which also hosts links to associated videos of the urethane molding process.

B. Proprioceptive Sensing

Proprioception is the ability of the body to know its configuration based on internal sensing of the musculoskeletal system. In this work, the robot's main drive actuators (Fig. 4) provide proprioception in terms of position encoder and load (current) values. These are standard measurable parameters in Dynamixel XM actuators. Video data is also recorded synchronously, but only for debugging purposes; it is not processed by the controller or learning algorithm. All control is performed open-loop, in the sense that we only provide joint position commands as ramp functions (as will be described in the next section) and do not measure object pose.

C. Control Approach

Our control approach makes use of the inherent torque (current) and position control modes of the Dynamixel Model-X actuators, which may be switched between at run-time. This enables the hand to maintain a stable grasp on the object as manipulation actions (such as rolling a square object between the fingers) are being executed, while also allowing the capability to adjust normal force application. This capability is beneficial to feature generation, as the same manipulation action by the position controlled finger tends to generate different position and load outputs from the torque controlled finger, when different objects are being manipulated. Please note that the controller is fully described in [17], but will be summarized here.

During object motion with our controller, the finger that is moving *towards* the object is placed in torque control mode, with a reference torque Γ_R. The other finger is placed in position control mode and leads the motion with a varying position reference (a ramp function). More explicitly, if both fingers are moving clockwise then the left finger (which is moving towards the object) will be in torque mode, as illustrated in Fig. 5. When the fingers move anti-clockwise, the roles will reverse. Note

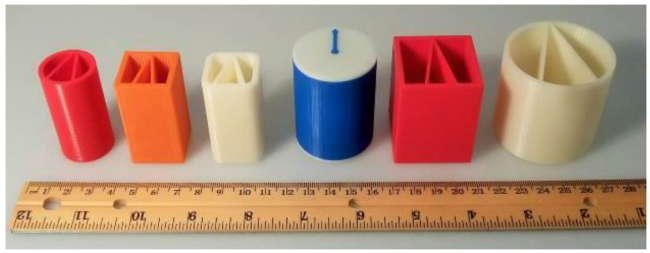

Fig. 5. The six manipulation objects, ordered by size. They are also described in Table I.

that a similar concept was applied to velocity and torque control of simple robot fingers for object manipulation in [29].

As the position controlled finger moves, the torque controlled finger attempts to maintain the constant torque reference Γ_R. This causes the fingers to sustain contact with the grasped object during motion, while also attempting to apply a constant normal force. The reference, Γ_R, may either be set as low (0.25 Nm) or high (1 Nm). This magnitude determines the normal force on the grasped object and therefore compression of the suspended low-friction surface, (Figs. 2 & 3). When a low-torque reference is provided, the low-friction surface of the VF finger will remain exposed during manipulation, enabling object sliding (Fig. 2 top right). If a high-torque reference is provided, the high resulting normal force will push the low-friction surface behind the high-friction surface, causing the VF finger to grip and/or roll the object.

IV. Methods

The goal of this study was to determine if proprioceptive actuator data from VF finger manipulations could be used to distinguish a variety of objects of different sizes and shapes, when automatically parsed without any prior associations by a machine learning based classifier.

For example, it is clear that variations in grasp aperture (the distance between fingers) during within-hand object manipulation should be able to allow discrimination between circular objects (which roll) and rectangular objects (which pivot and rotate). However, we provide the classifier with no kinematic calculations that converts raw actuator position to finger position, or associates the two actuator position variables together in a way that would lead to grasp aperture determination. This also applies to features related to actuator load, position error and associated time derivatives (as will be discussed in Section IV.B).

We therefore define the following task for the machine learning approach: given a large set of arbitrary, general and pre-defined proprioceptive features, select those which are most relevant to object classification.

A. Objects

The objects used for the test scenario are shown in Fig. 6 and described in Table I. All objects were 3D printed in ABS with a wall thickness of 2.5 mm. Note that particular attributes of shape and size were repeated between objects to focus investigations on whether the system would be better at differentiating either size or shape. These objects were manipulated in a planar fashion, with the robot hand supported above a flat surface on which the object rests before being manipulated (Fig. 1).

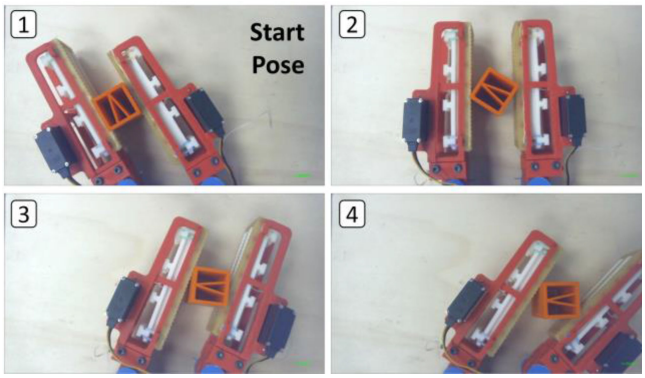

Fig. 6. One half-cycle of the object-rotation WIHM action used for proprioceptive data collection. For a full cycle, the fingers would return to the start pose.

B. Data collection

Though initial hopes were to use both sliding and rolling capabilities to explore objects through functional motion sequences. It was soon observed that certain cylindrical objects were often ejected from the hand following several sliding actions. Considering that this is an initial proof-of-concept study, it was decided that reliable baseline data from simple manipulations was preferable to data from more varied, but error-prone manipulations. A back-and-forth rolling action was therefore utilized as the exploratory procedure for this work (Fig. 6), following the initial positioning of the object into the start pose, which is achievable by sliding.

The rolling action is achieved by moving to the rightmost, then leftmost limits of the workspace while applying a high Γ_R value, causing the object to pivot. Fig. 1 shows the rolling being executed from left (panel 1) to right (panel 4) for the 25.4 mm (1 inch) square object. Following this, the motion is reversed and the object returned to the start pose. This constitutes one cycle. The object exploration was completed in four sets of seven cycles per object. Between each set the object was removed and replaced in roughly the same location in the gripper. This permitted some variation in starting conditions.

C. Recorded Data

Fig. 7 illustrates the captured data over one object rolling cycle with the 25.4 mm square object. The data consists of each actuator's position, position reference (demand), and load data. Note that the position reference signals are only followed by a finger when it is in position control mode, which we illustrate in Fig. 7 using a dotted line, with a solid line indicating that the actuator (and finger) is in torque controlled mode. Note also that, as described in Section III.C, the position-controlled and torque-controlled roles of the fingers switch depending on whether the object is being moved toward the left or right.

D. Gross Feature Extraction

Fig. 7 illustrates that the trajectories of position, position reference and load are approximately trapezoid profiles. This allows us to automatically extract features based on key aspects of these profiles, notably the 'elbows' of the trapezoids (which may also be considered as regions of significant gradient change). These 20 points (denoted A-T) are encoded in terms of time, magnitude, gradient (between points) and error (in the case of Position and Position Reference) as described in Table II. The time indices of the reference points in *position* and *position reference* (i.e., points A-C and D-F) are the same and therefore are only sampled once. Also, in order to capture the more subtle differences between trajectories, several waypoints between points were added for sampling (e.g., the gradient is sampled between M and N, but also sampled in the central 1/3rd of the trajectory between M and N).

This method provides a total of 66 'gross features' which are provided to the classifier. From these gross features, we will later extract 'key features', as will be discussed in Section V.B.

TABLE I
SIZE AND SHAPE CHARACTERISTICS OF THE SIX MANIPULATION OBJECTS

Object	Shape	Size	Diameter (mm)
1	Circle	Small	25.4
2	Circle	Medium	38.1
3	Square	Small	25.4
4	Square	Medium	38.1
5	R-Square	Small	25.4
6	Circle	Large	50.8

E. Machine Learning Approach

A total of 168 movement cycles were available for the 6 objects (28 cycles per object). Each cycle was represented by the 66 features previously described. The data was randomly split using *stratified 5-fold cross validation*. This split the trials so that 80% of the data was used for training, and the remaining 20% was used for testing the model. This splitting is completed 5 times and then the training is run 100 times, the classification accuracies converging to the presented classification value to follow.

For classifier selection, we implemented *TPOT* (Tree-based Pipeline Optimization Tool [43]), a machine learning pipeline that makes use of genetic algorithms to find the best classification model for the given data. From this analysis, we found the Extra Trees classifier (with 100 estimators), an extended version of the Random Forests classifier, presented the best cross validation results. For validation, we also tested a Random Forests classifier and a Support Vector Machine, which fell marginally short (about 5%) in classification accuracy compared to that of Extra Trees.

F. Classification Experiments

Three separate classification approaches were completed in order to identify how well the machine learning approach was able to distinguish between different properties of objects. These experiments are as follows:

A) Different size (but constant shape)
B) Different shape (but constant size)
C) Different shape and size

This involved separate training and testing of the classifiers with selected object data.

For experiment A, the system was trained and tested using only data from cylindrical shaped objects, in three different

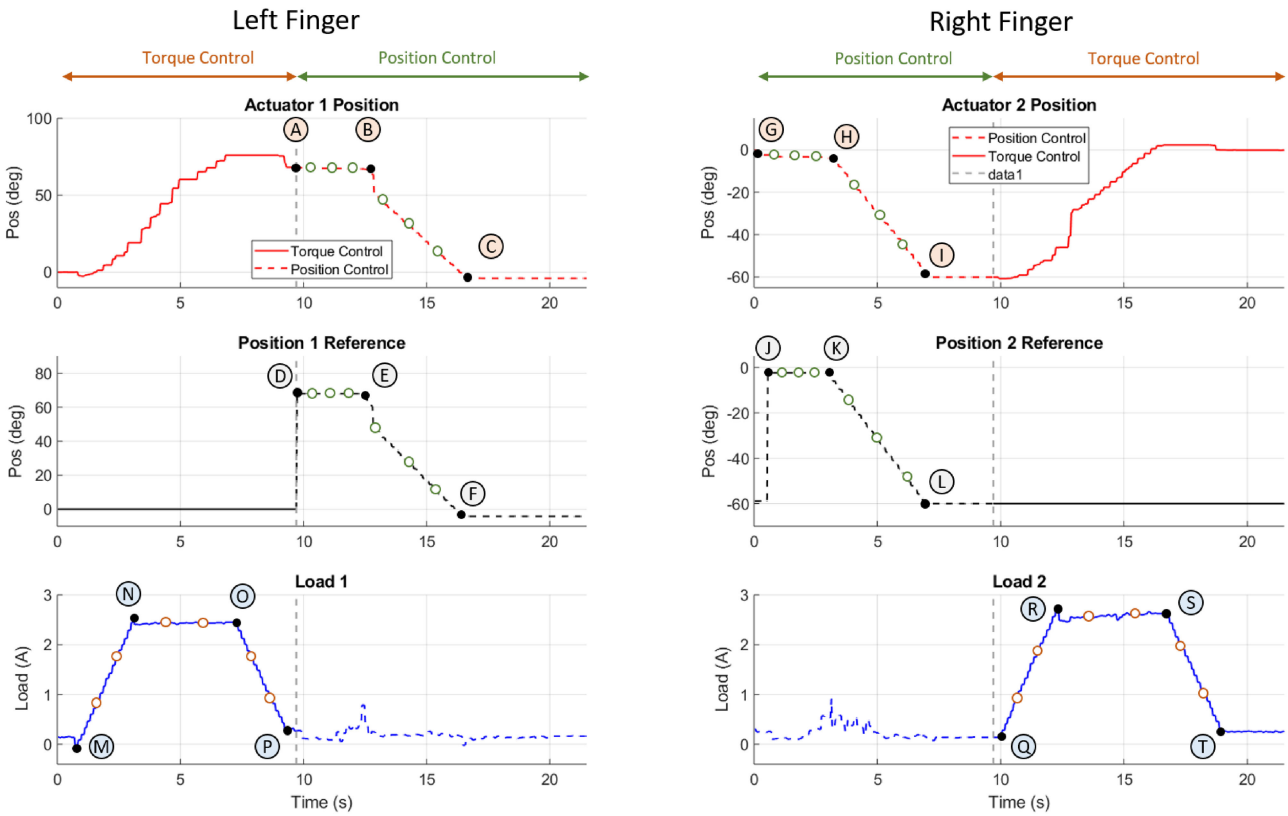

Fig. 7. Actuator Position, Position Reference (demand) and Load signals for one back-and-forth manipulation of the small square object. The manipulation changes direction at approximately 9.6 seconds. The labels A-T show events (specified by large changes in gradient) where values of time and magnitude were sampled to create the general set of 66 features. Additional features were created by taking the difference (between Position and Position Reference) or gradient (in the case of Load) in the intervals between the labels (illustrated by small circles). This process automatically generates 66 features to comprehensively describe the manipulation action, as further detailed in Table II.

sizes (diameters). These sizes are shown in Table I, but are referred to in the test as 'small, medium and large'.

For experiment B, three objects with different shapes (circle, square and rounded square) were selected with the same 'small' size (25.4 mm diameter).

For experiment C, which includes all objects, is the most difficult as certain objects resemble other objects at particular time instances. For example, when the medium size square object is in the middle of the rotation (i.e., held by opposing corners) the grasp aperture (space between the fingers) resembles that of the large circle. Additionally, the rounded square may resemble a circle or square at different points of the manipulation action.

V. Results

A. Gross Feature Classification

Using the Extra Trees classifier with parameters selected by the TPOT algorithm and all 66 features, the classification accuracies for the three experiments are displayed in Table III. While a classification rate of 89.8% was achieved for both the size and shape classification task (Experiment C), this rate rises when the classifier has only to predict one of these object parameters. These classification accuracies were therefore 90.4% for size distinction (experiment A) and 93.7% for shape (experiment B) distinction.

The confusion matrices associated with these experiments are presented in Fig. 8 (experiments A and B) and Fig. 10 (experiment C).

In experiment A, the classifier has the most difficulty with the small object, misclassifying it as a large object. This may be due to the reduction in manipulation workspace size that occurs with large objects. This has the effect of diluting other features.

Experiment B illustrates better classification accuracy, most likely due to different shape objects causing notable differences in actuator trajectories. This is highlighted in Fig. 9, which illustrates how square objects, with sharp corners, can cause sudden changes in actuator trajectories at certain points of the workspace.

This is apparent in the quite different range of finger and object trajectories that stem from rotation of a square (which pivot on its corners), the rounded square (which pivots to a less degree), and the circle (which rolls without pivoting). As a result, most of the errors in this experiment are caused by the system misclassifying the rounded square as a circle.

Finally, when the system trained on all of the objects in Table I (a variety of shapes and sizes) with all 66 features, the model makes the most errors when predicting rounded squares and large circles. Intuitively, we presumed that this classification would be the most difficult since we only have one

TABLE II
THE 66 GROSS FEATURES ARE CONSTRUCTED FROM A NUMBER OF MEASUREMENTS OF SEVERAL VARIABLES AT PRE-DEFINED EVENTS IN THE DATA (THOUGH THE TIMING OF THESE EVENTS CHANGES BETWEEN TRIALS). THESE MEASUEMENTS ARE ALSO ILLUSTRATED IN FIG. 7

Value	Points	Sub Points	Number of Features
Time	A-I, M-T	No	14
Magnitude	A-T	No	20
Gradient	MN, NO, OP, QR, RS, ST	No	6
Central Gradient	MN, NO, OP, QR, RS, ST	Yes	6
Error	AD-BE (5), BE-CF (5)	Yes	20
	GJ-HK (5), HK-KL (5)		
		Total	**66**

TABLE III
RESULTS OF THE THREE CLASSIFICATION EXPEIRMENTS WHEN USING ALL 66 FEATURES

Experiment	Test	Accuracy
A	Size	90.40%
B	Shape	93.70%
C	Size & Shape	89.80%

example of a large size object and one example of a rounded shape object. The classification of these two objects is therefore actually testing some of the interpolation and extrapolation of our learned model.

B. Key Feature Identification/Classification

Key features are features of the data that were determined to have the greatest contribution to overall classification accuracy. To determine key features we used an 'Importance' metric, which determines how much a feature contributes to the overall classification for an experiment. This importance metric was based on the Gini impurity measure, which was introduced in [44] and is often used in ensemble tree classifiers. When a random element in the data set is selected, the Gini impurity represents the likelihood of accurate classification given a random class selected from the distribution of labels. This measure is extracted for each feature when determining how to split the branches for each tree in the forest, which has the main intention of measuring purity of the node after a split.

The feature importance measure is then calculated by averaging the Gini measures for each split in the forest. We then characterize feature contribution by scaling the Gini impurities to add up to 100 and finding percentages. These percentages characterize how important a feature is to our learned model.

A complete set of importance values for all 66 features for a 'pilot' classification of experiment A's data is given in the Appendix. To create 'Key Feature' classifiers, we selected the top 6 features, i.e., those that contribute most to the classification of objects in each of the three experiments. These key features are provided in Table IV, where the letters coincides with the feature labels in Fig. 7.

Somewhat surprisingly, in all experiments the algorithm has selected the key features to only be position or position reference magnitudes. More specifically, it has not given much importance to any load, gradient, sub-points, errors or time index values (as described in Table II). Indeed, features of this

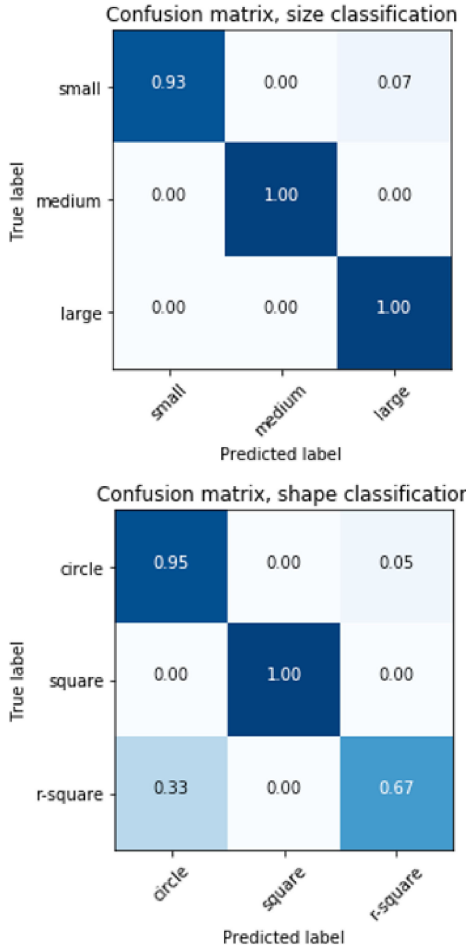

Fig. 8. Confusion matrices for experiments A (size classification) and B (shape classification).

kind can be seen to take much lower ranking in the table provided in the Appendix.

We believe that the importance of position based features is due to the adaptive nature of the grasping and manipulation scheme, where the torque based control of one of the fingers means that contact is always maintained with the object, regardless of object shape and size. Though manipulation with different shapes and sizes no doubt cause changes in load trajectories, such variations appear more subtle than the variations that occur in the positioning of the fingers over the span of the manipulation action.

Table V illustrates the classification accuracy that is achieved for each experiment when only limited numbers of key features are used. These results are presented for a range of classifiers that make use of between 6 and 1 key feature. This data is also represented in Fig. 11, along with the accuracy achieved when all features are used.

It is noticeable that the relationship between accuracy and feature number is non-linear in all of the experiments, with accuracy actually increasing in some occasions, when the number of features are reduced. This non-intuitive behavior is related to the randomness of the machine learning approach, which also does not consider the dependency that may occur between features. Nonetheless, reducing the number of features in experiment C (the most challenging

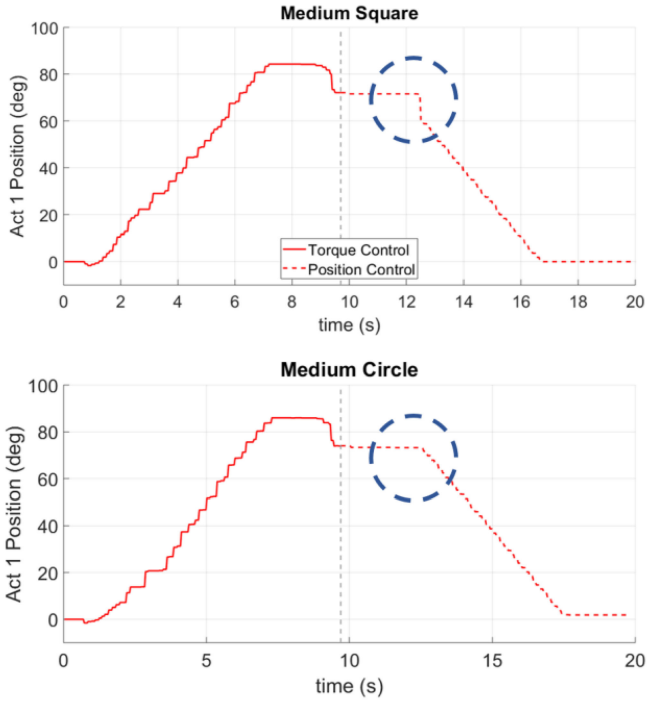

Fig. 9. Actuator 1 position recordings for two different rolling manipulations with a medium square (top) and medium circle (bottom). The change in trajectory caused by corner pivoting has been highlighted.

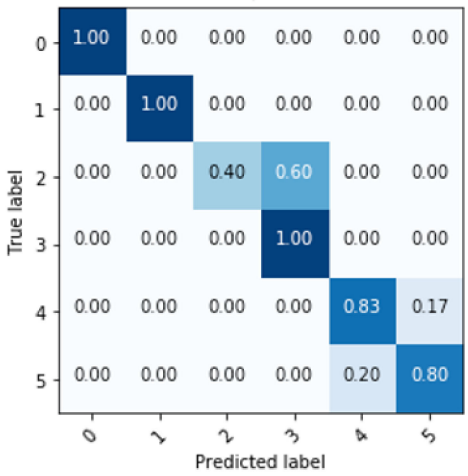

Object	Shape	Size
1	Circle	Small
2	Circle	Medium
3	Square	Small
4	Square	Medium
5	R-Square	Small
6	Circle	Large

Fig. 10. Confusion matrix for experiment C (size and shape classification) with key to object labels (object numbers are same as in Table I).

classification task) from 66 to 6 leads to a reduction of only 4% classification accuracy, while using only a single feature gives classification accuracy of over 80% for experiment A.

TABLE IV
KEY FEATURES AND IMPORTANCE MEASURES (IMP) FROM THE EXTRA TREES CLASSIFIER FOR EXPERIMENTS A, B, AND C. THE FEATURE NOTATIONS ARE REFERENED FROM FIG. 8. ALL KEY FEATURES REFERRING TO A POSITION VALUE HAVE BEEN SHADED GREY, WHILE UNSHADED FEATURES REFER TO POSITION REFERENCE VALUE. NOTE THAT NO KEY FEATURES WERE IDENTIFIED FROM ACTUATOR LOAD

Key	Experiment Features					
Feature	A	Imp (%)	B	Imp (%)	C	Imp (%)
1	G	8.57	B	8.14	G	6.08
2	J	7.69	D	7.97	B	6.02
3	L	5.24	G	6.78	J	5.71
4	I	5.06	H	6.27	D	5.69
5	K	5.04	J	5.53	H	5.01
6	D	3.91	A	5.40	A	5.00

Legend: I Position J Position Reference

TABLE V
CLASSIFICATION ACCURACY FOR EXPERIMENTS A, B, AND C GIVEN THE REDUCED FEATURES PRESENTED IN TABLE IV

Number of	Accuracy (%)		
Key Features	A	B	C
6	80.2	92.8	86
5	80.1	92.2	86.8
4	81.9	93.1	85.9
3	83.6	94	83.7
2	79.7	80	84.5
1	81.1	76.8	65.8

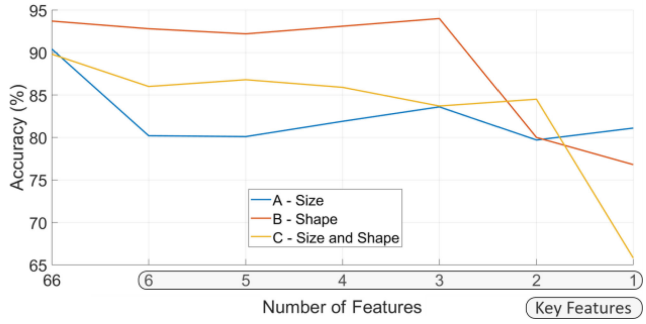

Fig. 11. Change in classification accuracy for all three experiments using all 66 features versus only one to six key features.

VI. CONCLUSION

This work introduces the concept of proprioceptive object sensing and discrimination using novel and mechanically simple 'Variable Friction' fingers capable of performing within-hand manipulation (WIHM). The simple but novel switching position/torque-based control method facilitates the extraction of haptic object data via active manipulation, as the gripper adaptively maintains contact with objects through manipulation actions, despite variations in size and shape. It is this adaptation that allows distinct manipulation data to be generated from rather simple within-hand exploratory manipulation actions that do not require explicit re-programming for different objects. This reflects a major goal of the VF finger design

methodology, which is to enable WIHM with low mechanical and control complexity, compared to related work in the field.

Due to the previously unexplored nature of the manipulation and control scheme, we deliberately did not hand-select features for our object classifier. Instead, we have taken an approach of automatically extracting a large number of features related to position, position-reference and load. Following initial classification of objects using all of the features (in three categories of size, shape and both), we subsequently were able to arrange the 66 features in order of importance. This enabled classification to be attempted again, but using only a heavily reduced number of automatically selected 'key features'. Notably, the experiments were performed again using only 1-6 key features.

It is worth noting that these key features were all automatically selected to have their origin either in the position trajectory of the actuators or in the position reference signals (Table V). Though it is somewhat surprising that actuator torque/load did not play a significant role in the key features. While the position controlled finger drives the motion of the gripper and object, the torque controlled finger demonstrates inherent compliance in order to maintain a grasp on the object during this motion. As a result, actuator torque has an indirect role in achieving our classification results, by adaptation of finger position trajectories with respect to the object size and shape, therefore leading to different actuator profiles for each object.

The classification results were promising at $\geq$90% accuracy when all 66 features were used, showing that there is potential for using a simple WIHM scheme for object classification, without the use of tactile sensors. Interestingly this accuracy remained about 80% for all experiments when only 6 features were used. Indeed, experiment A produced results that could still be considered satisfactory with only 1 feature, though this was not the case for the more challenging experiment C.

Overall, this work has provided an application of the recently developed VF fingers, showing their potential for haptic feature extraction via within-hand object manipulation without the requirement of force, torque or tactile sensors. As the VF fingers are open source and simple to fabricate, we hope that others are able to make use of the various properties of these manipulators. On the other hand, the approach presented in this paper is currently specific to the Model VF variable friction robot gripper. To our knowledge, this is the only variable friction hand in literature, and the only hand that uses such a controller for WIHM. The novelty of our robotic platform therefore makes consideration of a general approach to proprioceptive-based object classification difficult.

In the future, we wish to extend this work beyond the controlled geometric primitives of this study into more realistic and irregular objects manipulated three dimensional (rather than planar) workspaces. The robust handling of such objects, in addition to the capability of using sliding as well as rolling WIHMs for data gathering, are likely to be inherently linked to more complex and versatile variable-friction finger morphologies, probably consisting of multiple phalanges and/or additional fingers. Of course, the current control scheme will require modification to be compatible with these new finger designs while enabling more complex manipulation actions and richer proprioceptive data extraction.

APPENDIX
IMPORTANCE VALUES FOR ALL 66 GROSS FEATURES

Ranking	Variable Name	Category	Importance (%)
1	'pos2_value1',	Pos	6.66
2	'pos2_ref_value1',	Pos Ref	6.44
3	'pos1_value2',	Pos	6.25
4	'pos2_value2',	Pos	6.08
5	'pos1_ref_value2',	Pos Ref	5.19
6	'pos1_value1',	Pos	4.51
7	'pos1_ref_value1',	Pos Ref	4.22
8	'pos2_ref_value3',	Pos Ref	3.77
9	'pos2_ref_value2',	Pos Ref	3.75
10	'pos1_ref_value3',	Pos Ref	3.21
11	'pos2_value3',	Pos	2.95
12	'pos1_value3',	Pos	2.59
13	'pos1_diff_line1_3',	Pos Diff	2.48
14	'pos1_ref_index1',	Pos Ref Time	2.05
15	'pos1_diff_line1_4',	Pos Diff	2.01
16	'pos1_diff_line2_3',	Pos Diff	1.52
17	'pos1_diff_line1_2',	Pos Diff	1.44
18	'pos1_diff_line2_2',	Pos Diff	1.09
19	'load1_val1',	Load	1.06
20	'pos1_diff_line2_5',	Pos Diff	1.01
21	'load2_val1',	Load	0.99
22	'load2_mid_slope2',	Load Slope	0.97
23	'load2_index3',	Load	0.95
24	'load2_index2',	Load	0.90
25	'pos1_ref_index2',	Pos Ref Time	0.90
26	'pos1_diff_line2_4',	Pos Diff Line	0.89
27	'load1_index3',	Load	0.88
28	'load1_index1',	Load	0.88
29	'pos2_ref_index1',	Pos Ref Time	0.87
30	'load2_index1',	Load	0.85
31	'load1_val2',	Load	0.82
32	'pos2_diff_line2_3',	Pos Diff Line	0.82
33	'load1_val1',	Load	0.81
34	'pos2_diff_line2_4',	Pos Diff Line	0.79
35	'pos2_diff_line1_4',	Pos Diff Line	0.79
36	'pos1_diff_line1_5',	Pos Diff Line	0.78
37	'load2_val1',	Load	0.78
38	'pos2_diff_line1_1',	Pos Diff Line	0.77
39	'pos2_diff_line1_5',	Pos Diff Line	0.76
40	'pos2_diff_line1_3',	Pos Diff Line	0.75
41	'load1_mid_slope1',	Load Mid Time	0.73
42	'load2_val2',	Load	0.70
43	'pos1_ref_index3',	Pos Ref Time	0.69
44	'pos2_diff_line2_1',	Pos Diff Line	0.66
45	'load1_index4',	Load	0.66
46	'load2_mid_slope1',	Load Mid Time	0.65
47	'load2_index4',	Load	0.65
48	'load1_val1',	Load	0.63
49	'pos2_diff_line2_2',	Pos Diff Line	0.63
50	'pos2_ref_index2',	Pos Ref Time	0.62
51	'load1_mid_slope2',	Load Mid Time	0.60
52	'load2_val1',	Load	0.58
53	'pos1_diff_line2_1',	Pos Diff Line	0.57
54	'load2_full_slope2',	Load Full Time	0.56
55	'load2_mid_slope3',	Load Mid Time	0.55
56	'load1_full_slope2',	Load Full Time	0.55
57	'load1_full_slope1',	Load Full Time	0.55
58	'pos2_diff_line2_5',	Pos Diff Line	0.54
59	'load1_mid_slope3',	Load Mid Time	0.54
60	'load2_full_slope3',	Load Full Time	0.51
61	'pos2_diff_line1_2',	Pos Diff Line	0.49
62	'load1_index2',	Load	0.48
63	'pos2_ref_index3',	Pos Ref Time	0.43
64	'pos1_diff_line1_1',	Pos Diff Line	0.42
65	'load2_full_slope1',	Load Full Time	0.41
66	'load1_full_slope3']	Load Full Time	0.37

REFERENCES

[1] S. J. Lederman and R. L. Klatzky, "Extracting object properties through haptic exploration," *Acta Psychol. (Amst).*, vol. 84, pp. 29–40, 1993.

[2] V. Chu *et al.*, "Using robotic exploratory procedures to learn the meaning of haptic adjectives," in *Proc. IEEE Int. Conf. Robot. Autom.*, 2013, pp. 3048–3055.

[3] A. M. Okamura, M. L. Turner, and M. R. Cutkosky, "Haptic exploration of objects with rolling and sliding," in *Proc. Int. Conf. Robot. Autom.*, 1997, vol. 3, pp. 2485–2490.

[4] P. Dario *et al.*, "Planning and executing tactile exploratory procedures," in *Proc. IEEE/RSJ Int. Conf. Intell. Robot. Syst.*, 1992, pp. 1896–1903.

[5] Z. Su, J. a. Fishel, T. Yamamoto, and G. E. Loeb, "Use of tactile feedback to control exploratory movements to characterize object compliance," *Frontiers Neurorobot.*, vol. 6, pp. 1–9, 2012.

[6] J. Sinapov, C. Schenck, and A. Stoytchev, "Learning relational object categories using behavioral exploration and multimodal perception," in *Proc. IEEE Int. Conf. Robot. Autom.*, 2014, pp. 5691–5698.

[7] I. M. Bullock and A. M. Dollar, "Classifying human manipulation behavior," in *Proc. IEEE Int. Conf. Rehabil. Robot.*, 2011, pp. 1–6.

[8] N. Chavan-Dafle, R. Holladay, and A. Rodriguez, "In-hand manipulation via motion cones," *Robot. Sci. Syst.*, 2018. [Online]. Available: https://journals.sagepub.com/doi/10.1177/0278364919880257

[9] J. Shi, J. Z. Woodruff, P. B. Umbanhowar, and K. M. Lynch, "Dynamic in-hand sliding manipulation," *IEEE Trans. Robot.*, vol. 33, no. 4, pp. 778–795, Aug. 2017.

[10] N. Y. Chong, "A generalized motion/force planning strategy for multi-fingered hands using both rolling and sliding contacts," in *Proc. IEEE/RSJ Int. Conf. Intell. Robots Syst.*, 1993, pp. 113–120.

[11] R. S. Fearing, "Simplified grasping and manipulation with dextrous robot hands," *IEEE J. Robot. Autom.*, vol. 2, no. 4, pp. 188–195, Dec. 1986.

[12] T. Ishihara, A. Namiki, M. Ishikawa, and M. Shimojo, "Dynamic pen spinning using a high-speed multifingered hand with high-speed tactile sensor," in *Proc. 6th IEEE-RAS Int. Conf. Humanoid Robot.*, 2006, pp. 258–263.

[13] J. Ueda, M. Kondo, and T. Ogasawara, "The multifingered NAIST hand system for robot in-hand manipulation," *Mech. Mach. Theory*, vol. 45, no. 2, pp. 224–238, 2010.

[14] L. Biagiotti, F. Lotti, C. Melchiorri, and G. Vassura, "How far is the human hand ? a review on anthropomorphic robotic end-effectors basic concepts," *Hand*, p. 21, 2004. [Online]. Available: http://citeseerx.ist.psu.edu/viewdoc/summary?doi=10.1.1.104.7899

[15] H. van Hoof, D. Tanneberg, and J. Peters, "Generalized exploration in policy search," *Mach. Learn.*, vol. 106, no. 9/10, pp. 1705–1724, 2017.

[16] A. Delgado, C. A. Jara, and F. Torres, "Adaptive tactile control for in-hand manipulation tasks of deformable objects," *Int. J. Adv. Manuf. Technol.*, vol. 91, no. 9/12, pp. 4127–4140, 2017.

[17] A. Spiers, B. Calli, and A. Dollar, "Variable-friction finger surfaces to enable within-hand manipulation via gripping and sliding," *IEEE Robot. Autom. Lett.*, vol. 3, no. 4, pp. 4116–4123, Oct. 2018.

[18] F. E. Vina B., Y. Karayiannidis, K. Pauwels, C. Smith, and D. Kragic, "In-hand manipulation using gravity and controlled slip," in *Proc. IEEE Int. Conf. Intell. Robots Syst.*, 2015, pp. 5636–5641.

[19] D. L. Brock, "Enhancing the dexterity of a robot hand using controlled slip," in *Proc. IEEE Int. Conf. Robot. Autom.*, 1988, no. 7, pp. 249–251.

[20] A. A. Cole, P. Hsu, and S. S. Sastry, "Dynamic control of sliding by robot hands for regrasping," *IEEE Trans. Robot. Autom.*, vol. 8, no. 1, pp. 42–52, Feb. 1992.

[21] D. C. Chang and M. R. Cutkosky, "Rolling with deformable fingertips," in *Proc. IEEE/RSJ Int. Conf. Intell. Robot. Syst. Human Robot Interact. Cooperative Robot.*, 1995, pp. 194–199.

[22] X. Z. Zheng, R. Nakashima, and T. Yoshikawa, "On dynamic control of finger sliding and object motion in manipulation with multifingered hands," *IEEE Trans. Robot. Autom.*, vol. 16, no. 5, pp. 469–481, Oct. 2000.

[23] T. Yoshikawa, Y. Yokokohji, and A. Nagayama, "Object handling by three-fingered hands using slip motion," in *Proc. Int. Conf. Intell. Robots Syst.*, 1993, pp. 99–105.

[24] R. D. Howe and M. R. Cutkosky, "Practical force-motion models for sliding manipulation," *Int. J. Robot. Res.*, vol. 15, no. 6, pp. 557–572, Dec. 1996.

[25] S. Goyal and A. Ruina, "Planar sliding with dry friction Part 1. limit surface and moment function," *Wear*, vol. 143, pp. 307–330, 1991.

[26] N. Xydas, "Modeling of contact mechanics and friction limit surfaces for soft fingers in robotics, with experimental results," *Int. J. Robot. Res.*, vol. 18, no. 9, pp. 941–950, 1999.

[27] I. M. Bullock and A. M. Dollar, "A two-fingered underactuated anthropomorphic manipulator based on human precision manipulation motions," in *Proc. IEEE Int. Conf. Robot. Autom.*, 2016, pp. 384–391.

[28] W. G. Bircher, S. Member, A. M. Dollar, S. Member, N. Rojas, and M. Ieee, "A two-fingered robot gripper with large object reorientation range," in *Proc. IEEE Int. Conf. Robot. Autom* ., 2017, pp. 3453–3460.

[29] M. Yashima and T. Yamawaki, "Iterative learning control for whole-arm object manipulation through coordination of torque/velocity-controlled fingers," in *Proc. IEEE Int. Conf. Intell. Robot. Syst.*, 2015, pp. 6223–6230.

[30] A. J. Spiers, M. V. Liarokapis, B. Calli, and A. M. Dollar, "Single-grasp object classification and feature extraction with simple robot hands and tactile sensors," *IEEE Trans. Haptics*, vol. 9, no. 2, pp. 207–220, Apr./Jun. 2016.

[31] R. L. Klatzky and S. J. Lederman, "Identifying objects from a haptic glance.," *Perception Psychophys.*, vol. 57, no. 8, pp. 1111–1123, 1995.

[32] A. Spiers, S. Baillie, T. Pipe, and R. Persad, "Experimentally driven design of a palpating gripper with minimally invasive surgery considerations," in *Proc. IEEE Haptics Symp.*, 2012, pp. 261–266.

[33] R. L. Klatzky, J. M. Loomis, S. J. Lederman, H. Wake, and N. Fujita, "Haptic identification of objects and their depictions," *Perception Psychophys.*, vol. 54, no. 2, pp. 170–178, 1993.

[34] S. E. Tomlinson, R. Lewis, and M. J. Carre, "Review of the frictional properties of finger-object contact when gripping," *Proc. Institution Mech. Eng. Part J J. Eng. Tribol.*, vol. 221, no. 8, pp. 841–850, 2007.

[35] S. E. Tomlinson, R. Lewis, and C. M. J., "The effect of normal force and roughness on friction in human finger contact," *Wear*, vol. 267, no. 5/8, pp. 1311–1318, 2009.

[36] S. Comaish and E. Bottoms, "The skin and friction: Deviations from Amonton's laws, and the effects of hydration and lubrication," *Brit. J. Dermatol.*, vol. 84, no. 1, pp. 37–43, 1971.

[37] C. Chorley, C. Melhuish, T. Pipe, J. Rossiter, and G. Whiteley, "A biologically inspired fingertip design for compliance and strength," in *Proc. Towards Auton. Robot. Syst.*, 2008, pp. 239–244.

[38] M. J. Adams *et al.*, "Finger pad friction and its role in grip and touch," *J. Roy Soc. Interface*, vol. 10, no. 80, 2012, Art. no. 20120467.

[39] C. Chorley, C. Melhuish, T. Pipe, and J. Rossiter, "Development of a tactile sensor based on biologically inspired edge encoding," in *Proc. Int. Conf. Adv. Robot.*, pp. 1–6, 2009.

[40] P. Akella and M. Cutkosky, "Manipulating with Soft Fingers: Modeling Contacts and Dynamics," *Mech. Eng.*, pp. 764–769, 1989.

[41] M. Cutkosky, J. Jourdain, and P. Wright, "Skin materials for robotic fingers," in *Proc. IEEE Int. Conf. Robot. Autom.*, 1987, vol. 4, pp. 1649–1654.

[42] N. Xydas and I. Kao, "Modeling of contact mechanics and friction limit surfaces for soft fingers in robotics, with experimental results," *Int. J. Robot. Res.*, vol. 18, no. 9, pp. 941–950, 1999.

[43] R. S. Olson, R. J. Urbanowicz, P. C. Andrews, N. A. Lavender, L. C. Kidd, and J. H. Moore, "Automating biomedical data science through tree-based pipeline optimization," in *Proc. Eur. Conf. Appl. Evol. Comput.*, 2016, vol. 9597, pp. 123–137.

[44] L. Breiman, J. Friedman, C. Stone, and R. Olshen, *Classification and Regression Trees (Wadsworth Statistics/Probability)*. New York, NY, USA: CRC Press, 1984.

Adam J. Spiers received the B.Sc. degree in cybernetics and control engineering and the M.Sc. degree in engineering and information sciences from the University of Reading, Reading, U.K., in 2004 and 2006, and the Ph.D. degree in mechanical engineering from the University of Bristol, Bristol, U.K. He completed this work while employed as a Research Scientist with the Department of Mechanical Engineering, Yale University. He is currently a Research Scientist with the Haptic Intelligence Department, Max Planck Institute for Intelligent System, Stuttgart, Germany. His research focuses on human and robot movement, manipulation, and haptic sensing/perception.

Andrew S. Morgan (S'15) received the B.E. degree in computer engineering and the B.S. degree in computer science from Youngstown State University, Youngstown, OH, USA, in 2017, and the M.S. degree in mechanical engineering from Yale University, New Haven, CT, USA, in 2019. He is currently working toward the Ph.D. degree in engineering sciences in the Grablab under Prof. Aaron Dollar with Yale University. His research focuses on advancing dexterous manipulation capabilities with compliant grippers by leveraging mechanical properties and machine learning. His awards and honors include the National Science Foundation Graduate Research Fellowship Program and the Tau Beta Pi Graduate Fellowship.

Krishnan Srinivasan received the bachelor's degree in computer science and mathematics from Yale University, New Haven, CT, USA. He is currently working toward the Ph.D. degree with the Department of Computer Science, Stanford University, Stanford, CA, USA advised by Prof. Jeannette Bohg. His current research focuses on robot learning, control, and in-hand manipulation, and he is interested in safety and meta-learning.

Berk Calli received the Ph.D. degree from the Delft University of Technology, Delft, The Netherlands, where he worked on active sensing algorithms aimed at increasing success rates of robotic grasping algorithms. He is an Assistant Professor with the Computer Science Department and Robotics Engineering program, Worcester Polytechnic Institute (WPI), Worcester, MA, USA. Prior to WPI, he was a Post-Doc with Yale University Grab Lab, where he worked on vision-based dexterous manipulation with underactuated robotic hands. He also works on facilitating performance quantification methods for robotic manipulation, and is a founder of Yale-CMU-Berkeley (YCB) benchmarking project, which provides a platform for the robotic manipulation community to develop and share benchmarking protocols. His main research focus is robotic manipulation and its applications in various domains, such as waste recycling, assistive technologies and within-hand manipulation. His lab develops manipulation algorithms by combining techniques in computer vision, control theory, and machine learning.

Aaron M. Dollar (SM'06) received the B.S. degree in mechanical engineering from University of Massachusetts at Amherst, Amherst, MA, USA, in 2000, and the S.M. and Ph.D. degrees in engineering sciences from Harvard University, Cambridge, MA, in 2002 and 2007, respectively. He is currently a Professor of mechanical engineering and materials science with Yale University, New Haven, CT, USA. He is an Editor and the Co-founder of RoboticsCourseWare.org, an open repository for robotics pedagogical materials. His research interests include robotic grasping and manipulation, tactile sensing, prosthetics and rehabilitation robotics, and robot locomotion. He is an active member of the American Society of Mechanical Engineers and the American Society of Engineering Education.